Polyamine-mediated sensitization of *Klebsiella pneumoniae* to macrolides through a dual mode of action

Joshua M. E. Adams[1], Peri B. Moulding[1] and Omar M. El-Halfawy[1,2*]

[1] Department of Chemistry and Biochemistry, Faculty of Science, University of Regina, Regina, SK, S4S 0A2, Canada

[2] Department of Microbiology and Immunology, Faculty of Pharmacy, Alexandria University, Alexandria, 21521, Egypt

[*] **Correspondence: omar.el-halfawy@uregina.ca (O.M.E.)**

Running title: Uncovering new polyamine macrolide antibiotic adjuvants

Abstract

The chemical landscape bacteria encounter at the infection site could shape their stress and antibiotic responses; these altered responses are not typically detected in standard lab conditions. Polyamines are small molecules typically overproduced by the host during infection and have been shown to alter bacterial stress responses. We sought to determine the effect of polyamines on the antibiotic response of *Klebsiella pneumoniae*, a Gram-negative priority pathogen. Interestingly, putrescine and other natural polyamines sensitized *K. pneumoniae,* including pan-drug resistant and hypervirulent isolates, to azithromycin, a macrolide protein translation inhibitor typically used for Gram-positive bacteria. The synergy was further potentiated in the physiological buffer, bicarbonate. Chemical genomic screens suggested a dual mechanism whereby putrescine acts at the membrane and ribosome levels. Putrescine permeabilized both the outer and inner membranes of *K. pneumoniae* in fluorometric (NPN) and colorimetric (β-lactamase and β-galactosidase) assays. Further, mutants with chemically and genetically perturbed membranes exhibited a loss of putrescine-azithromycin synergy. Putrescine also inhibited protein synthesis in an *Escherichia coli*-derived cell-free protein expression assay simultaneously monitoring transcription and translation. Profiling the putrescine-azithromycin synergy against a combinatorial array of antibiotics targeting various ribosomal sites suggested that putrescine acts as tetracyclines targeting the 30S ribosomal acceptor site. Next, we exploited the natural polyamine-azithromycin synergy to uncover azithromycin adjuvants by screening a polyamine analog library. We discovered four azithromycin synergists with activity from the low micromolar range, sharing modes of action similar to putrescine. This work sheds light on the bacterial antibiotic responses under conditions more reflective of those at the infection site and provides a new strategy to extend the macrolide spectrum to drug-resistant *K. pneumoniae*.

Keywords: Polyamines; macrolides; putrescine; Gram-negative bacteria; antibiotic adjuvants

Introduction

Antimicrobial resistance (AMR) is an increasingly rising problem gravely impacting today's society. In 2019, there was an estimated 4.95 million deaths worldwide associated with bacterial AMR [1]. The AMR public health crisis prompted the World Health Organization (WHO) to issue a list of priority pathogens posing the most serious threat that requires urgent action; Gram-negative bacteria make up the majority of this list due to the limited therapeutic options available against these bacteria[2-4]. Unlike Gram-positive bacteria, the Gram-negative ones possess an outer membrane, an integral component of which are lipopolysaccharides (LPS), which constitutes a formidable barrier that prevents antibiotic permeation [5]. *Klebsiella pneumoniae* is one of the Gram-negative bacteria on the WHO priority pathogens list, gaining international concern due to the high prevalence of hypervirulent and drug resistant strains [4]. With the constant rise in AMR and the inadequate antibiotic drug discovery pipeline [6], there is a dire need for new strategies to combat Gram-negative resistant strains[1].

Bacteria encounter a myriad of chemicals at the infection site that may alter their antibiotic susceptibility and virulence [7, 8]. The potential effects of such chemicals are not typically captured in standard antibiotic susceptibility assays, whose conditions follow the guidelines issued by standardizing agencies such as the Clinical and Laboratory Standards institute (CLSI). Polyamines constitute an important class of chemicals present at the infection sites, especially since they are overproduced by the host during infection [9]. Natural polyamines, such as spermine, spermidine, and putrescine, are small polycationic molecules produced by almost all living organisms and are critical for their viability [10]. During infection, polyamine biosynthesis is upregulated in regenerating tissues of the host at the inflammatory and infection site; for example, polyamines accumulate in the lungs during pneumonia infections, suggesting a

role in suppressing infection [11-13]. Additionally, polyamines play an immunomodulatory role, where spermine exhibits macrophage suppression and anti-inflammatory activity [12]. The polyamine backbone structure consists of regularly spaced positive charges interrupted by hydrophobic hydrocarbon bridges; this unique structure allows polyamines to interact with various macromolecules [14]. Polyamines can stabilize nucleic acids and thus influence transcription, chromosomal structure, apoptosis, and protein synthesis [15-20]; they are involved in cell growth, differentiation, cell membrane stability and immune responses in humans [14, 15].

Polyamines are similarly involved in cellular homeostasis and stress response in bacteria [21]. They can also alter antibiotic susceptibility in a wide range of Gram-positive and Gram-negative bacteria [22-27]. For example, polyamines increased resistance of *Pseudomonas aeruginosa* and *Burkholderia cenocepacia* to antibiotics, including polymyxins and fluoroquinolones [23-25], and conversely increased the susceptibility of *Staphylococcus aureus* and enteric bacteria, such as *Escherichia coli*, to β-lactam antibiotics [26].

Macrolides are a class of antibiotics that target and inhibit protein synthesis via binding to the 23S portion of the 50S bacterial ribosome subunits[28]. Antibiotics in this class are highly prescribed due to their potency, low toxicity, and favourable pharmacokinetic properties, particularly their oral bioavailability [29-31]. Newer classes of macrolides, such as the azalide azithromycin, are clinically advantageous due to their extensive and rapid distribution into tissues and intracellular compartments yet minimal accumulation in fat and muscle [30]. Typically, macrolides are used to treat Gram-positive infections with less application in Gram-negative ones due to their poor penetration of the outer membrane [32]. However, macrolides show potency against Gram-negative bacteria albeit under certain infection-relevant conditions. For example, *E. coli* exhibit heightened sensitivity to macrolides in the presence of the physiologically relevant

86 buffer bicarbonate, which interferes with the proton motive force increasing transport of
87 macrolides through the inner membrane [33]. Understanding the effects of macrolides against
88 priority Gram-negative bacteria, such as *K. pneumoniae*, especially under host relevant
89 conditions, may expand their spectrum of activity to this group of bacteria where the clinical
90 need is high.

91 In this study, we show that polyamines sensitize *K. pneumoniae* to the macrolide
92 azithromycin. We determined the mechanism of this synergy, revealing both a membrane and
93 target-dependent effects. These observations prompted us to screen a collection of synthetic
94 polyamine analogs for macrolide adjuvants against *K. pneumoniae*, identifying micromolar
95 azithromycin synergists. Together, this work offers potential new antimicrobial strategies against
96 multi-drug resistant Gram-negative bacteria.

97

98 **Results and discussion**

99 **Natural polyamines synergize with azithromycin.**

100 We conducted checkerboard assays to test the effect of the polyamine putrescine on
101 azithromycin susceptibility in *K. pneumoniae* MKP103, a derivative of the clinical outbreak
102 isolate KPNIH1 lacking its carbapenemase-encoding gene [34]. Putrescine synergized with
103 azithromycin with a fractional inhibitory concentration index (FICI) of 0.47±0.01 (Fig 1A). FICI
104 ≤ 0.5 were interpreted as synergy, FICI > 4.0 as antagonism, and $0.5 <$ FICI ≤ 4.0 as additive,
105 indifference, or no interaction. This synergy matches previously reported polyamine-induced
106 macrolide sensitivity in another Gram-negative organism, *E. coli* [26]; the mechanism of such
107 interaction is unknown. The putrescine-azithromycin synergy reversed macrolide resistance of *K.*
108 *pneumoniae* MKP103; putrescine at 20 mM lowered the azithromycin MIC to below the CLSI

109 clinical breakpoint (Fig 1A). A bacterial strain is deemed sensitive to an antibiotic at MIC values
110 less than the clinical breakpoint, thus may become clinically used[35]. We also observed
111 azithromycin synergy with other natural polyamines (spermine and spermidine, Fig 1B-C).
112 Polyamine physiological levels vary but are generally within the millimolar range and are further
113 increased at the infection site upon infection [36, 37]; hence polyamines at the site of infection may
114 be sufficient to drive azithromycin synergy similar to what we observed *in vitro*.

115 The polyamine-azithromycin synergy was maintained across diverse *K. pneumoniae*
116 clinical isolates. We conducted putrescine-azithromycin checkerboard assays against the *K.*
117 *pneumoniae* diversity panel, comprising 100 clinical isolates collected from 63 facilities in 19
118 countries with an array of genotypic and phenotypic differences that span pan-sensitive, pan-
119 resistant, and hypervirulent lineages (Supplementary Table 1) [38]. We observed the putrescine-
120 azithromycin synergy in 78 isolates (Fig 1D), which lowered azithromycin MIC below the CLSI
121 breakpoint in 77 isolates (Supplementary Table 1; examples in Fig 1E). Notably, such synergy
122 was conserved across pan-sensitive to pan-drug-resistant isolates, including those encoding
123 carbapenemase, OXA, NDM, and CTX β-lactamases, Rmt(B,F,H) methyltransferases, MCR-1,
124 Tet(X), and ErmB, which drive resistance against carbapenems, β-lactams, aminoglycosides,
125 colistin, tetracyclines, and erythromycin, respectively (supplementary Table 1). On the other
126 hand, the putrescine-azithromycin combination showed additive effects in 22 isolates, which
127 harbour genes encoding the macrolide phosphotransferases Mph(A), Mph(B), and Mph(E)
128 (Supplementary Table 1).

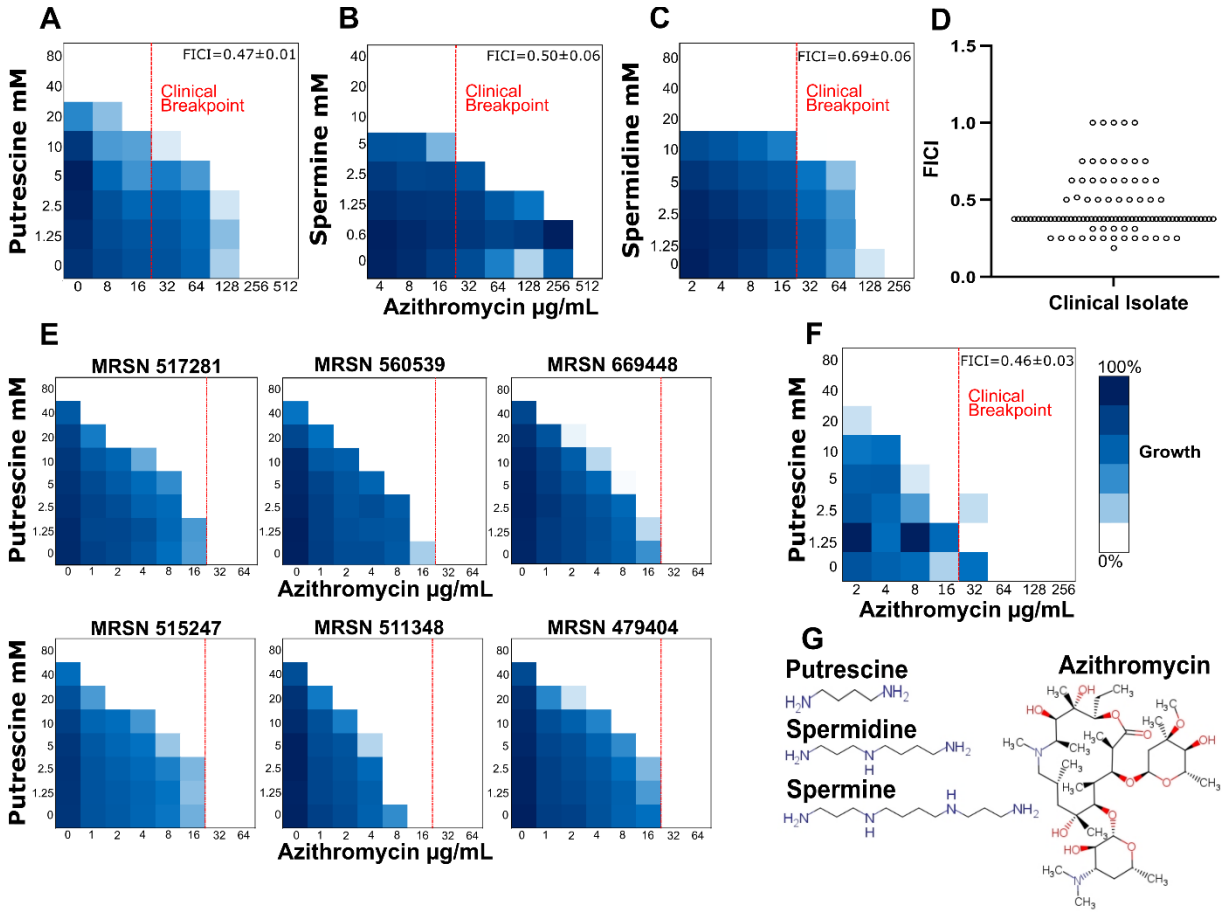

Figure 1. **Natural polyamines synergize with azithromycin against K. pneumoniae rendering it susceptible to the macrolide antibiotic.** A-C) Representative checkerboard assays of K. pneumoniae MKP103 of azithromycin combined with putrescine, spermine, and spermidine. D) A scatter plot representing the distribution of FICI values across the K. pneumoniae diversity panel. E) Representative checkerboard assays of select clinical isolates from the diversity panel. F) A checkerboard assay of putrescine and azithromycin against K. pneumoniae MKP103 in the presence of 25 mM bicarbonate buffer. G) Chemical structures of the polyamines used in this study and azithromycin. Dark blue regions represent high cell density determined by OD_{600}. Red dotted lines refer to the clinical breakpoint as set by CLSI. Mean of the FICI and SEM (standard error of the mean) are displayed on each representative checkerboard, n=3.

Next, we sought to test whether polyamines further sensitize *K. pneumoniae* to azithromycin in the presence of bicarbonate, the physiological buffer, in which Gram-negative bacteria are less resistant to macrolides [33]. We show that exposure to the physiological bicarbonate concentration (25 mM) resulted in 4-fold reduction in azithromycin MIC against *K. pneumoniae* (Fig 1F compared to 1A), as previously reported [33]. Putrescine further sensitized *K. pneumoniae* to azithromycin (further 16-fold reduction in MIC) in the presence of bicarbonate

146 (Fig 1F). These observations suggest that multiple physiologically-relevant factors may act in
147 tandem to alter bacterial responses to antibiotics.

148 **Genomic screens identify a dual mechanism of the polyamine-azithromycin synergy.**

149 To identify the mechanism of polyamine-azithromycin synergy, we hypothesized that a
150 mutant in the gene encoding the determinant of synergy will show increased azithromycin
151 susceptibility and loss in synergy with polyamines. We used an arrayed sequence-defined
152 transposon mutant library covering the non-essential genome of *K. pneumoniae* MKP103,
153 comprising one or multiple non-redundant mutants for each non-essential gene, with an average
154 of 2.5 mutants per gene [34]. First, we screened the library at two azithromycin sub-inhibitory
155 concentrations, 32 and 64 µg/mL, to identify mutants susceptible to azithromycin (Fig 2A-B and
156 Supplementary Fig 1). The screen revealed 71 mutants representing 67 genes showing partial or
157 complete growth inhibition at the sub-inhibitory azithromycin concentrations (Fig 2A-B and
158 Supplementary Fig 1). These genes include those whose products are involved in stress induced
159 mutagenesis (*recC* and *recB*), ribosomal function (*rpsO, rpsR, ybeY,* and *rsmB*), and membrane
160 integrity (*waaD, waaC, waaE, dsbA, acrB,* and *bamB*); knockouts of genes involved in these
161 functions have been previously identified in either *K. pneumoniae* or *E. coli* or both as more
162 susceptible to macrolides and other protein translation inhibitors [39-41].

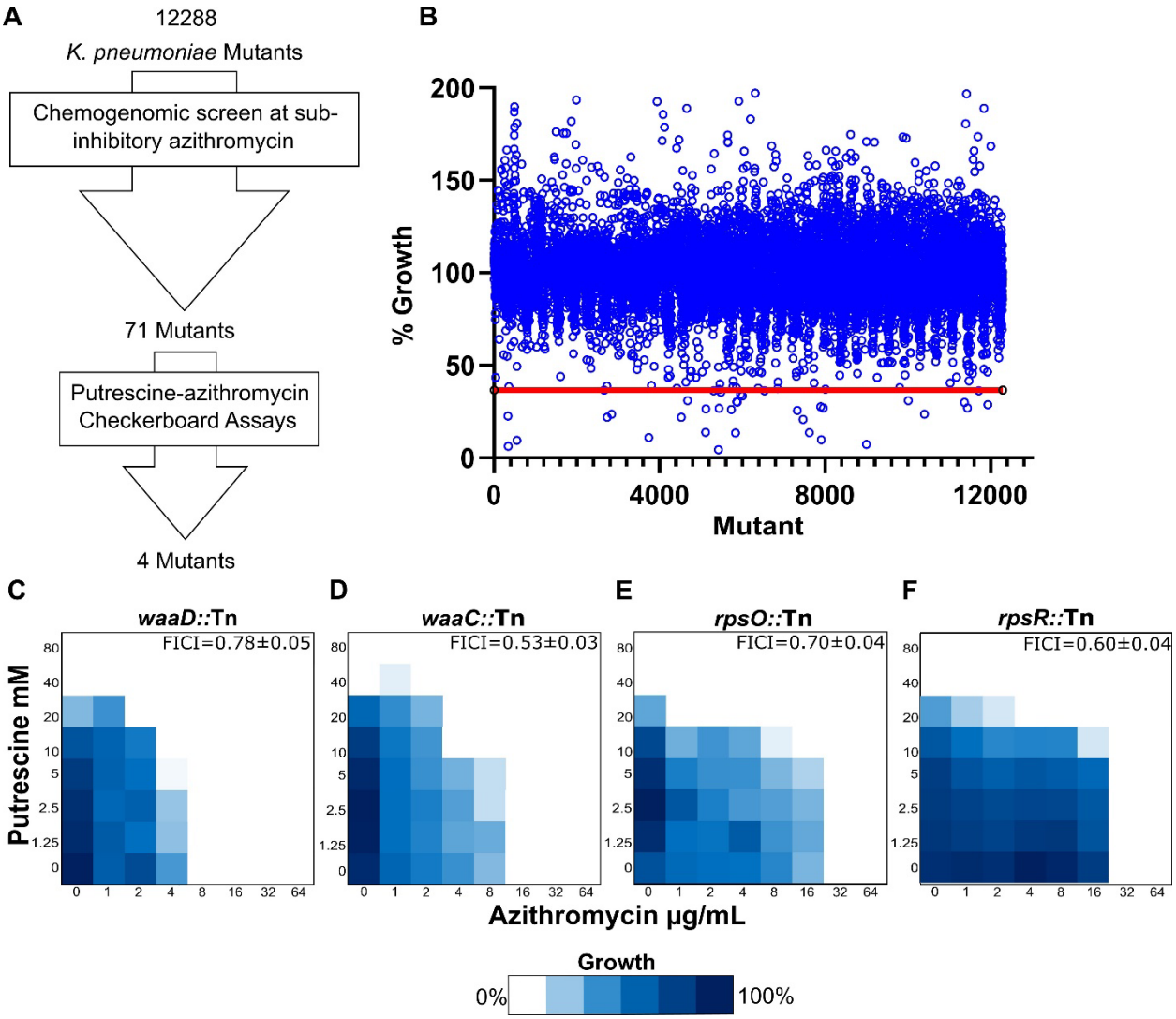

Figure 2**. A chemogenomic screen identifies putrescine-azithromycin synergy determinants.** A) A flow chart of the chemogenomic screen process that led to the identification of genetic determinants of azithromycin-putrescine synergy B) An index plot of the primary screen of *K. pneumoniae* MKP103 mutants grown in 32 µg/mL of azithromycin shown as % growth relative to that of the untreated mutants. Data points below a cut-off (the red line) of 1.5x the standard deviation of all datapoints below the interquartile mean are considered putative hits. C-F) Heat maps of representative putrescine-azithromycin checkerboards of the *K. pneumoniae* MKP103 mutants identified from the chemogenomic screen. Dark blue represents maximal growth determined by OD_{600}. Mean of the FICI and SEM are displayed on each representative checkerboard, n=3.

Next, we conducted putrescine-azithromycin checkerboard assays against the 71 mutants (Supplementary Fig 2 and Fig 2C-F). Azithromycin sensitivity (MIC ≤ 32µg/mL) and lack of synergy (FICI >0.5), suggested mutants of genetic determinants of the putrescine-azithromycin synergy; mutants with disruption in four genes (*waaD, waaC*, *rpsO,* and *rpsR*) fit these criteria

177 (Fig 2C-F). The disruptions in these mutants can be categorized into membrane (*waaD*::Tn and
178 *waaC*::Tn) and 30S ribosomal subunit (*rpsO*::Tn and *rpsR*::Tn) related disruptions.

179 Knockouts of *waaD* and *waaC* lead to the same deep rough LPS phenotype [42-44]. WaaD is
180 necessary for the production of ADP-L-glycero-D-mannoheptose, which WaaC incorporates into
181 the LPS structure; loss of these enzymes results in a truncated LPS without an outer core and
182 most of the inner core exposing Kdo2-lipid A (Supplementary Fig 3A-B)[42]. Notably, the
183 *waaD*::Tn was hypersensitive to novobiocin (Supplementary Fig 4), as expected for LPS deep
184 rough mutants [42, 45]. The azithromycin hypersensitivity of these *K. pneumoniae* mutants is in
185 agreement with previous reports of *E. coli* with a compromised LPS structure being more
186 sensitive to macrolides [39, 46]. Setting the azithromycin susceptibility cutoff to MIC ≤64μg/mL led
187 to the inclusion of *dsbA*::Tn, *bamB*::Tn, and KPNIH1_25560::Tn (predicted *waaE* [44]), which
188 exhibited partial loss of synergy (Supplementary Fig 2A-C and Supplementary Fig 3C). Loss of
189 DsbA leads to accumulation of inactive LptD (a lipopolysaccharide assembly protein), BamB is
190 a lipoprotein essential for assembly and insertion of β-barrel proteins into the outer membrane,
191 and WaaE is responsible for the transfer of the branch β-D-glucopyranose (Glc) to L-glycero-D-
192 manno-heptose I (Heptose I) [44, 47, 48]. Loss of *dsbA* and *waaE* has been previously shown to
193 exhibit macrolide sensitivity in *E. coli* and *K. pneumoniae,* respectively [41, 44], whereas knockouts
194 of *bamB* exhibit loss of a membrane barrier effect in *E. coli,* becoming sensitive to novobiocin [48].

195 We tested other mutants involved in LPS biosynthesis to determine the extent of LPS
196 truncation necessary for the loss of putrescine-azithromycin synergy. WaaF and WaaQ are
197 enzymes responsible for the sequential addition of heptose II and heptose III, respectively, to
198 complete the LPS inner core [44]. Knockouts of genes encoding both enzymes showed no change
199 in azithromycin MIC and retained putrescine-azithromycin synergy (Supplementary Fig 3D-E).

200 Together, a deep rough truncation of the LPS core leads to loss of putrescine-azithromycin
201 synergy, suggesting that a similar polyamine-mediated membrane permeabilization induces the
202 observed synergy (Supplementary Fig 3). For subsequent follow up assays, we used *waaD*::Tn as
203 a representative of the deep rough mutants.

204 The ribosomal proteins RpsO, RpsR, and RpsF create a complex within the platform
205 domain of the 30S ribosomal subunit, where RpsR and RpsF form heterodimers [49]. Both
206 *rpsO*::Tn and *rpsR*::Tn mutants exhibited an azithromycin MIC of 32 µg/mL and an FICI value
207 of 0.7 ± 0.04 and 0.6 ± 0.04, respectively (Fig 2G-H). RpsF is not represented in the *K.*
208 *pneumoniae* MKP103 library. The deletion of *rpsO* has been reported to influence the functional
209 capacity of 30S subunits and decrease the amount of 70S complexes [50]. RpsR is hypothesized to
210 be involved in the binding of aminoacyl-tRNA to the P site of the ribosome [51]. Genes encoding
211 other 30S ribosomal subunit proteins are essential except for *rpsA,* whose mutant yielded no
212 change in azithromycin susceptibility (data not shown). RpsA is weakly associated with the 30S
213 ribosome and even lacks association to the ribosome in some *E. coli* strains [52]. Notably, the
214 checkerboard of *infB*::Tn, a mutant of the translation initiation factor for *rpsO*, exhibited a partial
215 reduction in synergy and a 4-fold decrease in azithromycin MIC compared to that of the wild
216 type (Supplementary Fig 2D).

217 Together, our results suggest that polyamines synergize with azithromycin via a dual
218 mechanism of action: (1) increasing membrane permeability allowing azithromycin to cross this
219 barrier, and (2) acting on the 30S ribosomal subunit compounding the effects of azithromycin in
220 suppressing protein synthesis.

221 **Putrescine permeabilizes bacterial outer and inner membranes.**

222 Gram-negative bacteria, including *K. pneumoniae*, possess outer and inner membranes.
223 We studied the effects of polyamines on both membranes. Starting with the outer membrane, we
224 showed, in kinetic 1-*N*-phenylnaphthylamine (NPN) fluorometric assays, that putrescine
225 disrupted the outer membrane of *K. pneumoniae* shown as an increase in NPN uptake (Fig 3A).
226 A disruption of the outer membrane occurs at 10 mM and 20 mM of putrescine ($P < 0.0001$),
227 which is within the synergistic range of the putrescine-azithromycin interaction. Such putrescine-
228 mediated outer membrane perturbation was similar to that displayed by the deep rough LPS
229 mutant *waaD*::Tn, which showed a similar increase in NPN uptake relative to the wild type ($P <$
230 0.005, Fig 3B). *Salmonella enterica* serovar Typhimurium and *E. coli waaD* deletion mutants
231 also showed a similar (2 to 5-fold) increase in NPN uptake in comparison to the respective parent
232 strains [53, 54]. Using colorimetric quantification of the hydrolysis of nitrocefin, a β-lactam probe,
233 by a periplasmic β-lactamase constitutively expressed from pBR322 as another proxy for outer
234 membrane perturbation, we further confirmed the increased outer membrane permeability of the
235 *waaD*::Tn mutant in comparison to its parent strain (Fig 3C), in agreement with previous reports
236 [55].
237 Given that outer membrane permeabilization of the deep rough mutant (Fig 3B-C) is
238 sufficient to enable macrolides to cross that barrier (Fig 1A, Fig 2C-D, [39]), further membrane
239 perturbation may not lead to enhancement of the macrolide activity. Thus, the lack of putrescine-
240 azithromycin synergy in *waaD*::Tn further suggests that the polyamine-mediated outer
241 membrane perturbation contributes to the synergy. As such, we reasoned that chemically or
242 genetically perturbing the membrane should exhibit increased susceptibility to azithromycin and
243 a loss of synergy with putrescine, similar to *waaD*::Tn. Chemically perturbing *K. pneumoniae*
244 membrane by 1 μg/mL of polymyxin B nonapeptide (PMBN), a cationic peptide that disrupts the

245 outer membrane with little to no antimicrobial activity [56], led to a 4-fold decrease in
246 azithromycin MIC (Fig 3 D-E), consistent with previous reports [5, 56, 57], and a loss of putrescine-
247 azithromycin synergy (FICI 0.83 ± 0.10) (Fig 3E). Similarly, an *E. coli* with a compromised
248 outer membrane genetically-induced by the deletion of 9 efflux pump transmembrane proteins
249 (Δ9 mutant) [58], exhibited an 8-fold decrease in azithromycin MIC and a loss in synergy (FICI =
250 1.00 ± 0.00) relative to its parent strain (M6394), which showed a synergistic phenotype (FICI =
251 0.41 ± 0.07) (Supplementary Fig 5A-B). The *E. coli* wild type and Δ9 mutant showed NPN
252 profiles (Supplementary Fig 5C) similar to those of *K. pneumoniae* MKP103 wild type and
253 *waaD*::Tn (Fig 3B).

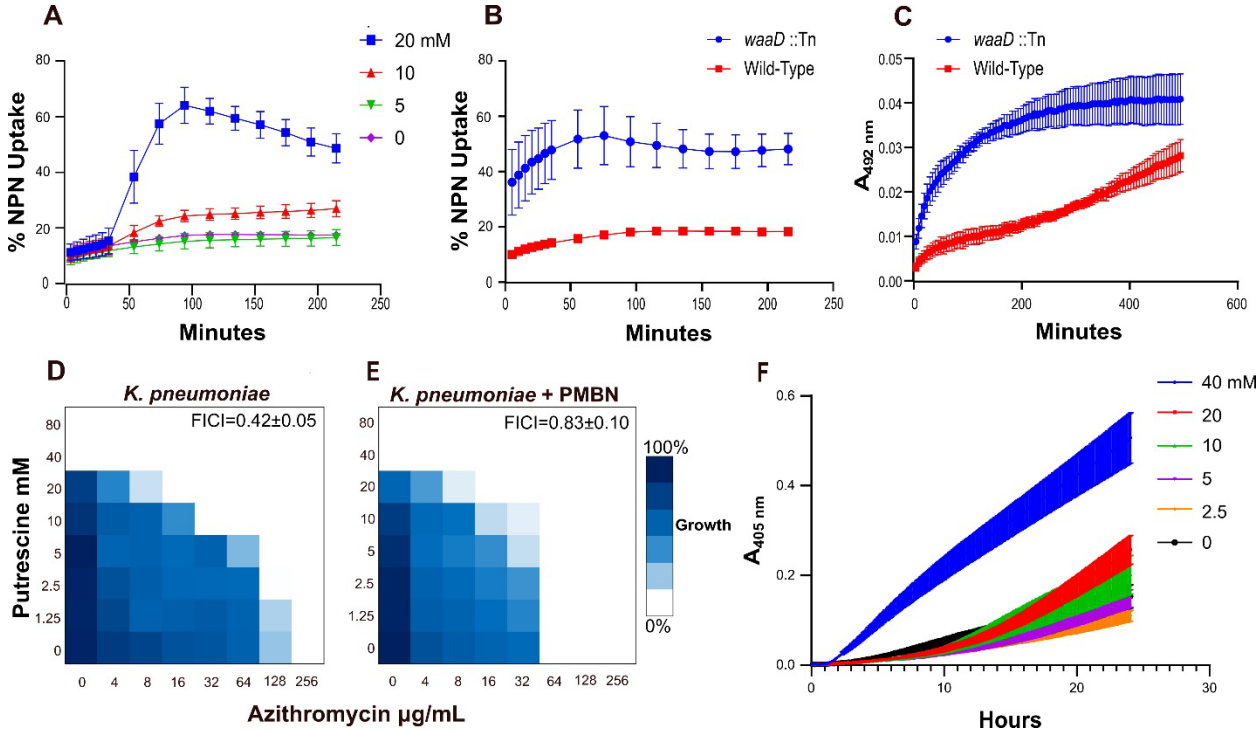

254

255 Figure 3. **Putrescine permeabilizes the outer and inner membranes of *K. pneumoniae* to azithromycin.** A-B)
256 Fluorometric kinetic assays displaying % NPN uptake in wild type *K. pneumoniae* MKP103 treated with different
257 concentrations of putrescine (A) and in *K. pneumoniae waaD*::Tn relative to its parent MKP103 strain (B). C) A
258 kinetic absorbance assay displaying nitrocefin hydrolysis by a periplasmic β-lactamase in *K. pneumoniae* wild type
259 and *K. pneumoniae waaD*::Tn. D-E) Representative checkerboards of putrescine-azithromycin combination against
260 *K. pneumoniae* MKP103 in the absence (D) and presence (E) of 1 µg/mL polymyxin B nonapeptide; dark blue
261 regions represent high cell density determined by OD_{600}. F) A kinetic absorbance assay of ONPG hydrolysis in *E.*
262 *coli* ML-35 as a proxy for inner membrane perturbation. All kinetic assays are the combined data of three

263 independent assays each done in triplicate. All error bars denote SEM. Mean of the FICI and SEM are displayed on
264 each representative checkerboard, n=3.
265

266 Notably, spermidine and spermine at the micromolar range have been reported to confer
267 resistance to polymyxin B in *P. aeruginosa* by localizing at the outer membrane. Molecular
268 dynamics simulations of model bacterial outer membranes have shown that polyamines engage
269 in electrostatic interactions with negatively charged phosphate groups, stabilizing the outer
270 membrane with the largest stabilizing effects in the order of spermidine, spermine, then
271 putrescine [59]. The activity of putrescine at the outer membrane in *K. pneumoniae* at the
272 physiologically relevant millimolar range has not been previously reported. At low putrescine
273 concentrations, we confirmed that putrescine can stabilize the outer membrane shown as reduced
274 NPN uptake relative to the untreated cells (Supplementary Fig 6). As such, it appears that
275 putrescine displays a dose-dependent activity on the outer membrane, ranging from stabilization
276 at low concentrations to disruption at higher concentrations.

277 The inner membrane of Gram-negative bacteria may constitute a second physical barrier
278 for azithromycin. We sought to test if putrescine also affects the inner membrane by measuring
279 the β-galactosidase-mediated o-nitrophenyl-β-D-galactopyranoside (ONPG) hydrolysis in a
280 lactose permease-deficient *E. coli* that constitutively expresses a cytoplasmic β-galactosidase (*E.*
281 *coli* ML-35). Putrescine at 40 mM significantly increased ONPG hydrolysis ($P < 0.0001$, Fig
282 3F), suggesting that polyamines can also disrupt the inner membrane, potentially contributing to
283 increasing intracellular azithromycin concentration. Taken together, we have shown evidence
284 that putrescine permeabilizes both the outer and inner membranes, contributing to its synergy
285 with azithromycin.

286 **Polyamines act on the ribosome compounding the protein synthesis inhibitory effect of**
287 **azithromycin.**

288 The lack of azithromycin-putrescine synergy in the 30S ribosomal subunit mutants
289 (*rpsO*::Tn and *rpsR*::Tn, Fig 2E-F) suggests the synergy may be driven, at least in part, by an
290 interaction between both molecules at the ribosomal level. Hence, we sought to test the effect of
291 putrescine on protein translation. To this end, we used a cell-free protein synthesis system, an
292 extract-based transcription/translation system derived from *E. coli* designed to synthesize
293 proteins under the control of T7 RNA Polymerase. We quantified the levels of a plasmid-
294 encoded destabilized enhanced Green Fluorescent Protein (deGFP) fluorometrically in the
295 presence and absence of putrescine (Fig 4 and Supplementary Fig 7). Simultaneously, we
296 measured the effects on transcriptional activity in real-time (Fig 4 and Supplementary Fig 7A-C),
297 since the plasmid also included a malachite green mRNA aptamer allowing for such
298 measurement fluorometrically via binding of malachite green dye [60]. At the higher tested
299 concentration of putrescine, mRNA levels were reduced but protein synthesis was further
300 inhibited (Supplementary Fig 7A-F). Similar reduction in gene expression has been previously
301 observed in cell-free *in vitro* gene expression models at high spermine and spermidine
302 concentrations [61]. Thus, to determine the effect of putrescine on protein synthesis due to a
303 ribosomal effect, the deGFP signal was normalized by the mRNA signal (Fig 4). The lower
304 putrescine concentrations exhibited increased protein synthesis (in the first ~90 minutes of
305 exposure, Fig 4), which is in agreement with previous reports that low concentrations of
306 polyamines promote protein synthesis in cell free systems [61]. A majority of intracellular
307 polyamines exist as polyamine-RNA and polyamine-ribosome complexes with evidence
308 suggesting they contribute to transcription and translation, playing an essential role in ribosome
309 biogenesis, tRNA positioning on the ribosome, and translation elongation speed [62-65]. Cross-
310 linking studies showed that ribosomes have >500 stably linked polyamines per ribosome, and it

311 has been suggested polyamine binding happens in a stochastic manner [65, 66]. On the other hand,
312 our results show that 80 mM of putrescine marked a significant decrease in protein synthesis,
313 suggesting a decreased ribosomal function of the cell-free protein expression system (P=0.0001,
314 Fig 4). The addition of spermine to ribosome complexes was previously shown to slow down
315 protein expression, inhibit peptidyl transferase activity, and possibly alter ribosome conformation
316 [67, 68].

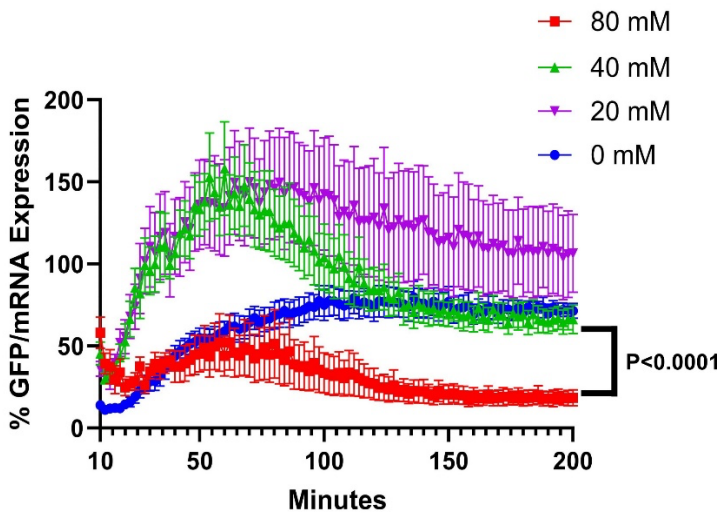

317

318 Figure 4. **Putrescine inhibits protein synthesis**. Protein (deGFP) and mRNA levels were simultaneously monitored
319 fluorometrically (433/475 and 610/650 nm, respectively) in black 384 well plates using the NEBExpress™ cell-free
320 protein expression system in 200 mM HEPES buffer with an engineered plasmid encoding deGFP with a malachite
321 green mRNA aptamer. Results shown are normalized by dividing each well's RFU deGFP value by the malachite
322 green RFU value and converted into a percentage of the maximal signal observed in the untreated condition. Raw
323 RFU data found in supplementary Fig 7A-F. All error bars denote SEM. A one-way ANOVA analysis followed by a
324 Brown-Forsythe and Welch test assessed the significance of the difference as indicated on the plot.
325

326 Next, we sought to determine the potential target site of putrescine within the ribosome
327 through a phenotypic combinatorial approach using antibiotics targeting different ribosomal sites
328 and a control (rifampicin) acting outside the ribosome. We hypothesize that, in the wild type,
329 antibiotics targeting the same site within the ribosome as that of putrescine will show similar
330 macrolide synergy as that of putrescine-azithromycin combination. Additionally, we hypothesize
331 that a compound that mirrors the phenotype of putrescine-azithromycin will show additive

332 effects when in combination with putrescine. We tested eight antibiotics, including azithromycin,
333 in combination with one another and with putrescine to compare their FICI values (Fig 5A).
334 These antibiotics targeted various sites within the ribosome: Paromomycin and gentamicin bind
335 to the aminoacyl site within the 30S ribosomal subunit leading to misreading of genetic code.
336 Chloramphenicol binds to the aminoacyl site of the 50S ribosomal subunit and prevents peptidyl
337 transferase. Azithromycin and erythromycin both block the 50S ribosomal subunit nascent
338 peptide tunnel inhibiting transpeptidation. Tetracycline and doxycycline target the 30S ribosomal
339 acceptor site preventing the association of aminoacyl-tRNA with the ribosome complex and
340 prevent mRNA binding [69]. We used rifampicin, an RNA polymerase inhibitor, as a control. Out
341 of the seven antibiotics tested, only tetracyclines (tetracycline and doxycycline) synergized with
342 azithromycin as putrescine did (Fig 5A). Synergy between the tetracycline doxycycline and
343 azithromycin has been observed before in *P. aeruginosa*, albeit the underlying mechanism has
344 not been resolved [70]. Checkerboard assays of putrescine-azithromycin combinations were
345 phenocopied by tetracycline-azithromycin combinations in the *K. pneumoniae* wild type strain
346 (Fig 5B-C) and tetracycline also showed additive effects with putrescine (Fig 5D). Similarly, the
347 additive effects of the putrescine-azithromycin combination against the ribosomal mutants
348 *rpsO*::Tn and *rpsR*::Tn was also observed in the tetracycline-azithromycin combination (Fig 5E-
349 H). Additionally, the combination of tetracycline and azithromycin, in checkerboards of PMBN
350 treated *K. pneumoniae* (FICI 0.50 ± 0.00) and the *waaD*::Tn mutant still exhibited significant
351 synergy (FICI 0.41 ± 0.07) (Supplementary Fig 8A-C); under these conditions, while the outer
352 membrane is perturbed chemically or genetically, synergy may still occur at the ribosomal level.
353 Previously, *E. coli* serially passaged in sub-lethal putrescine concentrations evolved
354 putrescine-resistant mutants that had truncations of the S7 30S ribosomal protein, a protein that

355 organizes the folding of the 3' major domain of 16S rRNA and crosslinks to the anticodon loop
356 of tRNAs [71, 72]. These mutants exhibited increased growth rates relative to the wild type when
357 grown in the presence of putrescine [72]. Indeed, adaptive resistance is likely to occur at the target
358 for a compound, supporting our findings that putrescine may act on the 30S ribosomal subunit.
359 Polyamine cross-linking in the 30S subunit leads to 16S rRNA structural changes [66]; similarly,
360 tetracycline has been shown to alter the structure of 16S rRNA [73]. Moreover, 30S subunits
361 lacking RpsO exhibit subtle changes in 16S rRNA nucleotide reactivity [50, 74]. Thus, it is probable
362 that the mutants of RpsO and RpsR lead to an altered 16S rRNA structure similar to that
363 occurring as a result of polyamine and tetracycline binding to the 30S subunit, which may
364 explain the lack of synergy of these drugs with azithromycin in *rpsO*::Tn and *rpsR*::Tn mutant
365 backgrounds. Together, our results provide support that putrescine acts on the 30S ribosomal
366 subunit similar to tetracycline and that it mediates the macrolide synergy via a dual mechanism
367 (at the membrane and ribosomal levels).

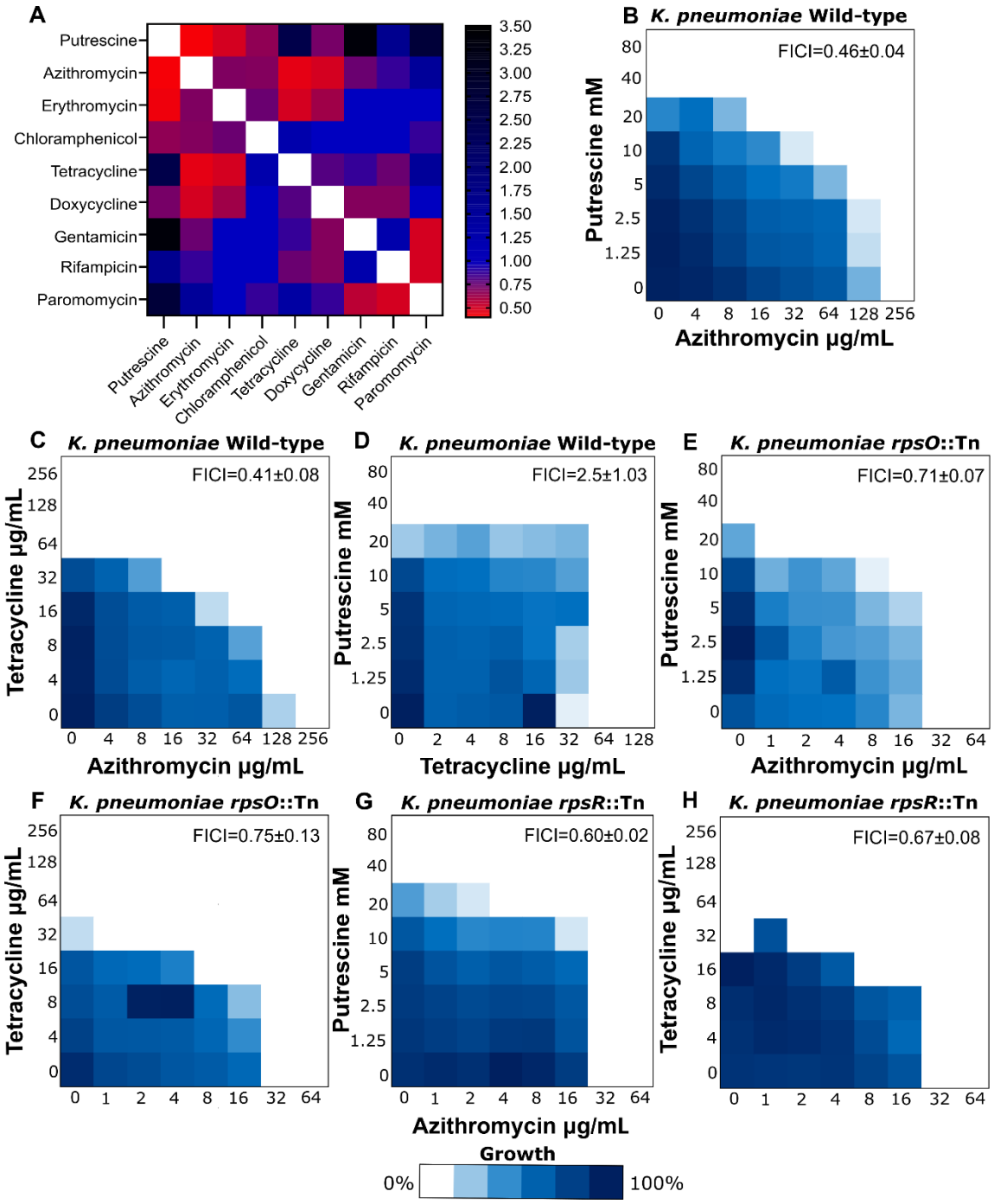

Figure 5**. Putrescine may inhibit the ribosomal 30S subunit in a similar manner as tetracyclines.** A) Heat map showing the average FICI value of duplicate checkerboard assays against *K. pneumoniae* MKP103 with various drug combinations. B-D) Checkerboard assays against *K. pneumoniae* (MKP103) treated with B) putrescine-azithromycin, C) tetracycline-azithromycin, and D) putrescine-tetracycline combinations. E-F) Checkerboard assays against *K. pneumoniae rpsO*::Tn treated with E) putrescine-azithromycin and F) tetracycline-azithromycin. G-H) Checkerboard assays against *K. pneumoniae rpsR*::Tn treated with G) putrescine-azithromycin and H) tetracycline-azithromycin. Dark blue regions represent high cell density determined by OD_{600}. FICI mean and SEM, derived from 3 independent experiments, are displayed on each representative checkerboard.

378 **A screen of a polyamine analog library uncovers azithromycin synergists.**

379 We sought to exploit the polyamine-azithromycin synergy and the understanding of its
380 mode of action to uncover an antibiotic adjuvant that may expand the spectrum of azithromycin
381 to *K. pneumoniae*. We hypothesized that a synthetic polyamine analog may lead to synergy with
382 azithromycin similar to that mediated by natural polyamines, serving as a potential macrolide
383 adjuvant. To this end, we screened a library of 86 polyamine analogs against MKP103 alone and
384 in combination with a sub-inhibitory concentration (1/8th MIC) of azithromycin (Fig 6A). Six
385 compounds displayed growth inhibition alone and in combination with azithromycin. Follow up
386 checkerboard assays of the six primary hits revealed that OES2-017, OES2-046, OES2-045, and
387 OES2-008 synergized with azithromycin at concentrations starting at the low micromolar range
388 with FICI values of 0.54 ± 0.11, 0.32 ± 0.05, 0.37 ± 0.03, and 0.29 ± 0.05, respectively (Fig 6B-
389 E). Similar to putrescine, the identified polyamine analogs showed growth inhibitory effects
390 against *K. pneumoniae* MKP103; their MIC values (31.25 μM, 2.5, 2.5, and 5 mM for OES2-
391 017, -045, -046, and -008, respectively, Fig 6B-E) were substantially lower than that of
392 putrescine (40 mM).

393 Next, we sought to identify the mechanism of azithromycin synergy by these four
394 compounds, first by checking if they acted through a similar mechanism as that of putrescine.
395 Therefore, we conducted checkerboard assays of each compound with azithromycin against the
396 *rpsO*::Tn, *rpsR*::Tn, and *waaD*::Tn *K. pneumoniae* mutants, against which putrescine lost its
397 synergy with the macrolide antibiotic, and tested their outer and inner membrane
398 permeabilization effects. Both OES2-017 and OES2-008 showed reduced or complete loss of
399 azithromycin synergy against all three mutants (Supplementary Fig 9A-F). Conversely, OES2-
400 045 and OES2-046 exhibited no loss of synergy against the mutants, except that the extent of the

401 synergy against *waaD*::Tn (mean FICI= 0.419 and 0.489, respectively) was reduced relative to
402 that against the wild type (mean FICI= 0.325 and 0.375, respectively) (Supplementary Fig 9G-
403 L). We showed in NPN fluorometric kinetic assays that OES2-017, OES2-008, OES2-045, and
404 OES2-046, in descending order of magnitude, disrupted the outer membrane of *K. pneumoniae*
405 in a dose dependant manner across the synergistic range of each compound (Supplementary Fig
406 10A-D). Further, all four analogs exhibited inner membrane activity, in colorimetric ONPG
407 hydrolysis assays against *E. coli* ML-35, in a dose dependant manner across the synergistic range
408 of each compound (Supplementary Fig 11A-D). Taken together, these results suggest that OES2-
409 017 and OES2-008 synergize with azithromycin via mechanisms similar to those of putrescine at
410 the ribosome and outer and inner membranes levels, whereas OES2-045 and OES2-046 may
411 exert their azithromycin synergy through membrane activity only. Importantly, these analogs
412 synergize with azithromycin at substantially lower concentrations than putrescine, serving as
413 potential macrolide adjuvants.

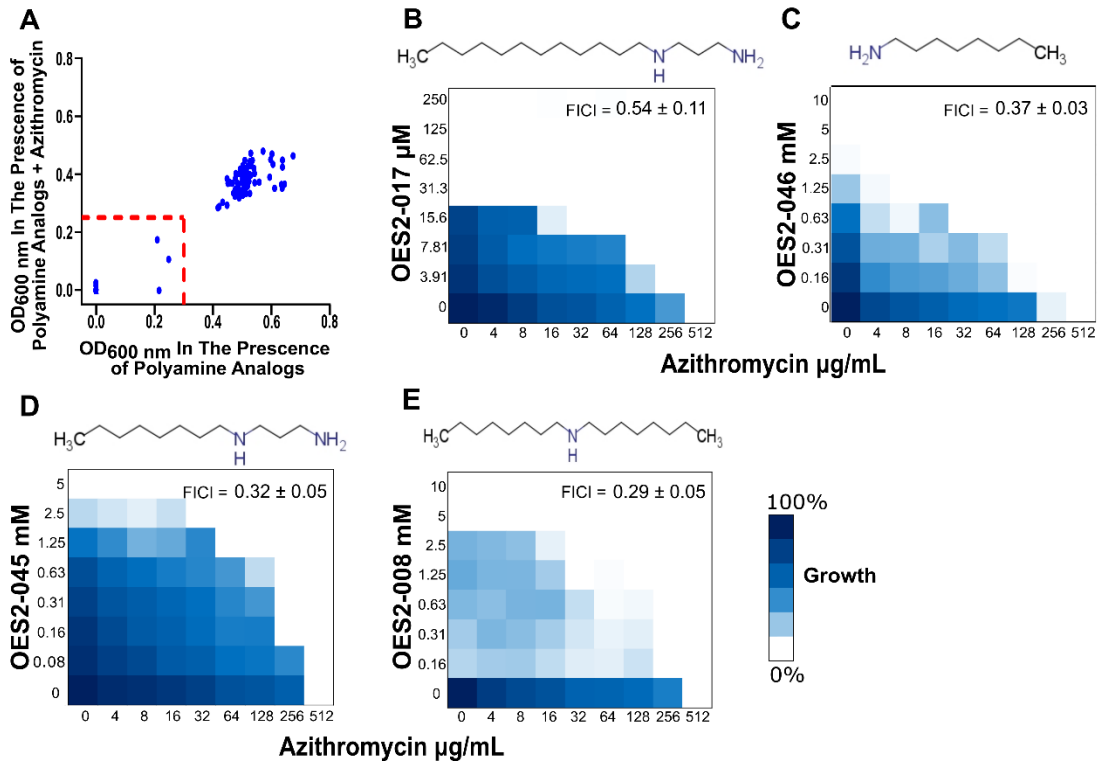

Figure 6. **Screening for azithromycin adjuvants identifies polyamine analogs with more potent azithromycin synergy and growth inhibitory activities.** A) A replica plot displaying the OD readings of *K. pneumoniae* MKP103 in the presence of the polyamine analogs at 2.5 mM alone (x-axis) and in combination with 64 µg/mL azithromycin (y-axis). B-E) Representative checkerboard assays of *K. pneumoniae* MKP103 treated with the prioritized polyamine analog hits in combination with azithromycin. All FICI values are shown as the average of at least 3 independent repeats and the SEM. Dark blue regions represent high cell density determined by OD_{600}.

Conclusions

In this study, we uncovered a sensitization of *K. pneumoniae* to the macrolide azithromycin in the presence of potentially physiological levels of polyamines. We showed that the putrescine-azithromycin synergy occurs in pan-drug-resistant and hypervirulent *K. pneumoniae* lineages, bringing azithromycin susceptibility in 78 of 100 clinical isolates below the CLSI breakpoint. Further, we have provided evidence towards a dual mechanism of action underlying the putrescine-azithromycin synergy, whereby the polyamine: 1. permeabilized the outer and inner membranes to azithromycin and 2. compounded the protein synthesis inhibiting effects of azithromycin by acting at the ribosome, likely at the 30S subunit.

431 Further, we discovered four synthetic polyamine analogs that displayed growth inhibitory
432 effects and synergy with azithromycin against *K. pneumoniae*, with greater potency compared to
433 natural polyamines. Synergy with currently available Gram-positive specific antibiotics, such as
434 macrolides, including by perturbing the Gram-negative outer membrane, represents a potential
435 strategy to combat drug-resistant Gram-negative bacteria [57]. As such, the polyamine analogs
436 discovered herein may broaden the spectrum of azithromycin, serving as a potential strategy to
437 combat antimicrobial resistant *K. pneumoniae*.
438

439 **Methods**

440 **Strains, reagents, and culture conditions.** Table 1 lists bacteria and plasmids used in this work.
441 Bacteria were grown in cation-adjusted Mueller Hinton medium (CAMHB, herein referred to as
442 MHB) at 37 °C buffered with 100 mM Tris-HCl pH7.4 buffer (to offset the alkalinity of higher
443 polyamine concentrations), unless otherwise indicated. Antibiotics and reagents were obtained
444 from Sigma unless otherwise indicated.

445 **Table 1. Bacterial strains and plasmids used in this study.**

Bacterial Strain	Description	Reference
K. pneumoniae		
MKP103	A derivative of the clinical outbreak isolate KPNIH1 lacking its carbapenemase-encoding gene	34
MKP103 Library	An arrayed sequence-defined transposon mutant library covering the non-essential genome of *K. pneumoniae* MKP103	34
K. pneumoniae Diversity Panel	A *K. pneumoniae* diversity panel, comprising 100 clinical isolates – Received from BEI resources	38
MKP103 pBR322	MKP103 transformed with pBR322	This study
MKP103 *waaD*::Tn pBR322	MKP103 *waaD*::Tn transformed with pBR322	This study

E. coli		
M6394	Wild-type GC4468 Δ(argF-lac)169 λ− IN(rrnD-rrnE)1 rpsL179 (Strr)	58
M6394 Δ9	M6394 Δ*acrB* Δ*acrD* Δ*acrEF*::spc Δ*emrB* Δ*emrY* Δ*entS*::cam Δ*macB* Δ*mdtC* Δ*mdtF*	58
ML-35 pBR322	$lacZ^{+}Y^{-}I^{-}$, *E. coli* with constitutive expression of β-galactosidase but lacking the lactose permease ML-35 with periplasmic β-lactamase	75
Bacterial Plasmids		
pBR322	Plasmid encoding a periplasmic β-lactamase	76
PT7-deGFP-Mgapt	pIVEX2.3d with a transcription unit of PT7:deGFP-Mgapt:T7term	60

446

447 **Antimicrobial susceptibility testing.** All MIC and checkerboard assays were conducted
448 following the CLSI method for MIC testing by broth microdilution [77]. The assays were
449 conducted in polystyrene 96-well plates with final volume of 100 µL/well and inoculum size
450 adjusted as optical density at 600 nm (OD_{600}) of 0.001. Plates were incubated while shaking at
451 600 RPM and 37°C; growth of the bacterial culture was determined by OD_{600} measurement at 24
452 hours. To assess the combined antimicrobial activity, fractional inhibitory concentration indices
453 (FICI) were calculated as $FICI = A/MIC_A + B/MIC_B$. A and B represent the MIC of the drugs
454 while in combination. MIC_A and MIC_B represent the individual MIC of each drug alone. FICI
455 values less than or equal to 0.5 were considered synergism, values greater than 4 were
456 considered antagonism, and values between 0.5 and 4 were indicated indifference, additive, or no
457 interaction.

458 **Arrayed transposon *Klebsiella pneumoniae* MKP103 library screen.** Overnight cultures of
459 the *K. pneumoniae* MKP103 library[34] were performed using the BioMatrix benchtop robot (S&P
460 robotics) into 384 well-density plates containing MHB with 150 µg/mL of chloramphenicol and
461 incubated at 37°C for 24 hours. Subsequently, the entire library was inoculated into MHB with

462 azithromycin at 32 μg/mL and 64 μg/mL and without azithromycin. The plates were incubated at
463 37°C, and OD_{600} was read after 24 hours.
464 **NPN assays.** The outer membrane permeability of *K. pneumoniae* MKP103 and *E. coli* M6394
465 wild type and mutants was measured using NPN uptake assays as previously described [78].
466 Briefly, bacteria were subcultured in MHB until mid to late log phase, washed, and resuspended
467 in either 100 mM Tris-HCl (pH 7.4) with 20 mM glucose or 5 mM HEPES (pH7.4) with 20 mM
468 glucose. The latter buffer was used only when low putrescine concentrations, causing minimal
469 pH changes, were tested. NPN was added to the bacterial suspension at a final concentration of
470 20 μM and dispensed into black 96 well plates pre-seeded with a concentration gradient of
471 putrescine to a total final volume of 200 μL. We tested untreated bacteria suspended in the same
472 buffer adjusted to the final pH reached upon addition of each tested putrescine concentration as a
473 negative control (untreated pH control) used to correct for any pH related signal. Fluorescence
474 was read kinetically (excitation λ=355 nm, emission λ=420 nm) every 5 minutes for 215
475 minutes. The %NPN uptake was calculated using the following equation: %NPN uptake = $(F_{obs}$-
476 $F_0)/(F_{100}-F_0)$ x 100, where F_{obs} is the observed fluorescence at a given concentration of
477 putrescine, F_0 is the fluorescence in non-treated cells (untreated pH control), and F_{100} is the
478 fluorescence of NPN in 8 μg/mL colistin-treated cells (used as a positive control).
479 **β-lactamase assay.** The outer membrane integrity of *K. pneumoniae* wild type and *waaD*::Tn
480 mutant were tested by measuring β-lactamase activity with nitrocefin hydrolysis as previously
481 described [79]. First, we extracted pBR322 from an *E. coli* strain carrying the plasmid (Monarch
482 Mini-Prep kit, NEB) and transformed it into electrocompetent *K. pneumoniae* strains of interest
483 by electroporation[34] Overnight cultures of *K. pneumoniae* pBR322 and *K. pneumoniae waaD*::Tn
484 pBR322 were diluted 100-fold into TSB and incubated at 37°C until late log phase (OD_{600} of

485 ~1.8). Aliquots of the sub-cultures were centrifuged and washed twice with PBS then
486 resuspended in 100 mM Tris-HCl buffer (pH 7.4) at a final OD_{600} of 0.01. The bacterial
487 suspensions mixed with 30 μM nitrocefin were dispensed into 96 well plates pre-seeded with the
488 tested drugs with a total final volume of 100 μL/well. The plates were incubated at 37°C while
489 measuring the absorbance kinetically at 492 nm every 10 minutes.
490 **β-galactosidase assay.** The inner membrane integrity of *E. coli* ML-35 pBR322 was tested by
491 measuring β-galactosidase activity with ONPG hydrolysis as previously described [79]. An
492 overnight culture of *E. coli* ML-35 pBR322 was diluted 100-fold into TSB and incubated at
493 37°C until late log phase (OD_{600} of ~1.8). Aliquots of the sub-culture were centrifuged and
494 washed twice with PBS then resuspended in 100 mM Tris-HCl buffer (pH 7.4) at a final OD_{600}
495 of 0.01. The bacterial suspensions mixed with 1.5 mM ONPG were dispensed into 96 well plates
496 pre-seeded with the tested drugs with a total final volume of 100 μL/well. The plates were
497 incubated at 37°C while measuring the absorbance kinetically at 405 nm every 2 minutes.
498 **Cell free protein expression.** An NEB Express Cell-free *E. coli* protein synthesis system (New
499 England Biolabs) was used for *in vitro* protein expression. Transcription and translation were
500 measured fluorometrically (excitation/emission wavelengths at 610/650 nm MGapt, 485/525 nm
501 deGFP) using an engineered plasmid that encodes a deGFP protein and a malachite green RNA
502 aptamer (PT7-deGFP-MGapt was a gift from Richard Murray, via Addgene plasmid # 67741;
503 http://n2t.net/addgene:67741) [60]. The cell-free protein synthesis system reaction mixture was
504 prepared following the manufacturer's protocol and dispensed as 5 μL aliquots into black 384
505 well plates. Putrescine, dH_2O, plasmid (124 ng/μL final concentration), and Malachite green dye
506 (10 μM final concentration) top up the reaction mixture reaching a combined final volume of 11
507 μL.

508 **Polyamine analog library screen.** *K. pneumoniae* MKP103 was inoculated in MHB with 100
509 mM Tris-HCl buffer (pH 7.4) at a 0.001 OD_{600} and dispensed into 96 well plates at a total final
510 volume of 100 µL (including polyamine analogs, azithromycin, vehicle, or combinations
511 thereof). Polyamine analogs were screened at 2.5 mM alone and in combination with 64 µg/mL
512 azithromycin. Plates were incubated at 37°C and 600 RPM; growth of the bacterial culture was
513 determined by OD_{600} readings at 24 hours.
514 **Statistical analysis.** All statistical analyses were calculated using GraphPad Prism 9.
515

516 **Acknowledgements.**
517 This work was funded by a Natural Sciences and Engineering Research Council of Canada
518 discovery grant, a Saskatchewan Health Research Foundation establishment grant, and startup
519 funds from the Faculty of Science at the University of Regina. O.M.E. holds a Canada Research
520 Chair in Chemogenomics and Antimicrobial Research. P.B.M. was supported by a CIHR CGS-
521 M award.

522 **References**

523 (1) Antimicrobial Resistance, C. Global burden of bacterial antimicrobial resistance in 2019: a systematic
524 analysis. *Lancet* **2022**, *399* (10325), 629-655. DOI: 10.1016/S0140-6736(21)02724-0.
525 (2) Nikaido, H. Molecular basis of bacterial outer membrane permeability revisited. *Microbiol Mol Biol*
526 *Rev* **2003**, *67* (4), 593-656. DOI: 10.1128/MMBR.67.4.593-656.2003.
527 (3) Ak, O.; Batirel, A.; Ozer, S.; Çolakoğlu, S. Nosocomial infections and risk factors in the intensive care
528 unit of a teaching and research hospital: a prospective cohort study. *Med Sci Monit* **2011**, *17* (5), Ph29-
529 34. DOI: 10.12659/msm.881750.
530 (4) WHO. Global Priority List of Antibiotic-Resistant Bacteria to Guide Research, Discovery, and
531 Development of New Antibiotics. world health organization: 2017.
532 (5) Delcour, A. H. Outer membrane permeability and antibiotic resistance. *Biochimica et Biophysica Acta*
533 *(BBA) - Proteins and Proteomics* **2009**, *1794* (5), 808-816. DOI: 10.1016/j.bbapap.2008.11.005.
534 (6) WHO. *Antibacterial agents in clinical development: an analysis of the antibacterial clinical*
535 *development pipeline*; 2019.
536 (7) El-Halfawy, O. M.; Valvano, M. A. Chemical Communication of Antibiotic Resistance by a Highly
537 Resistant Subpopulation of Bacterial Cells. *Plos One* **2013**, *8* (7). DOI: 10.1371/journal.pone.0068874.
538 (8) Perry, E. K.; Meirelles, L. A.; Newman, D. K. From the soil to the clinic: the impact of microbial
539 secondary metabolites on antibiotic tolerance and resistance. *Nat Rev Microbiol* **2022**, *20* (3), 129-142.
540 DOI: 10.1038/s41579-021-00620-w.
541 (9) Zhang, M.; Wang, H.; Tracey, K. J. Regulation of macrophage activation and inflammation by
542 spermine: a new chapter in an old story. *Crit Care Med* **2000**, *28* (4 Suppl), N60-66.
543 (10) Agostinelli, E.; Arancia, G.; Vedova, L. D.; Belli, F.; Marra, M.; Salvi, M.; Toninello, A. The biological
544 functions of polyamine oxidation products by amine oxidases: perspectives of clinical applications.
545 *Amino Acids* **2004**, *27* (3-4), 347-358. DOI: 10.1007/s00726-004-0114-4.
546 (11) Bjelakovic, G.; Stojanovic, I.; Jevtovic Stoimenov, T.; Pavlovic, D.; Kocic, G.; Rossi, S.; Tabolacci, C.;
547 Nikolic, J.; Sokolovic, D.; Bjelakovic, L. Metabolic correlations of glucocorticoids and polyamines in
548 inflammation and apoptosis. *Amino Acids* **2010**, *39* (1), 29-43.
549 (12) Zhang, M.; Wang, H.; Tracey, K. J. Regulation of macrophage activation and inflammation by
550 spermine: A new chapter in an old story. *Critical Care Medicine* **2000**, *28* (4), N60-N66.
551 (13) Liao, C. P.; Lasbury, M. E.; Wang, S. H.; Zhang, C.; Durant, P. J.; Tschang, D.; Lee, C. H. Inflammatory
552 cells are sources of polyamines that induce alveolar macrophage to undergo apoptosis during
553 Pneumocystis pneumonia. *J Eukaryot Microbiol* **2006**, *53 Suppl 1*, S134-135. DOI: 10.1111/j.1550-
554 7408.2006.00203.x.
555 (14) Gugliucci, A. Polyamines as clinical laboratory tools. *Clin Chim Acta* **2004**, *344* (1-2), 23-35. DOI:
556 10.1016/j.cccn.2004.02.022.
557 (15) Larque, E.; Sabater-Molina, M.; Zamora, S. Biological significance of dietary polyamines. *Nutrition*
558 **2007**, *23* (1), 87-95.
559 (16) Feuerstein, B. G.; Pattabiraman, N.; Marton, L. J. Spermine-DNA interactions: a theoretical study.
560 *Proc Natl Acad Sci U S A* **1986**, *83* (16), 5948-5952. DOI: 10.1073/pnas.83.16.5948.
561 (17) Feuerstein, B. G.; Pattabiraman, N.; Marton, L. J. Molecular dynamics of spermine-DNA interactions:
562 sequence specificity and DNA bending for a simple ligand. *Nucleic Acids Res* **1989**, *17* (17), 6883-6892.
563 DOI: 10.1093/nar/17.17.6883.
564 (18) Feuerstein, B. G.; Pattabiraman, N.; Marton, L. J. Molecular mechanics of the interactions of
565 spermine with DNA: DNA bending as a result of ligand binding. *Nucleic Acids Res* **1990**, *18* (5), 1271-
566 1282. DOI: 10.1093/nar/18.5.1271.
567 (19) Davis, R. H.; Morris, D. R.; Coffino, P. Sequestered end products and enzyme regulation: the case of
568 ornithine decarboxylase. *Microbiol Rev* **1992**, *56* (2), 280-290. DOI: 10.1128/mr.56.2.280-290.1992.

(20) Miyamoto, S.; Kashiwagi, K.; Ito, K.; Watanabe, S.; Igarashi, K. Estimation of polyamine distribution and polyamine stimulation of protein synthesis in *Escherichia coli*. *Arch Biochem Biophys* **1993**, *300* (1), 63-68. DOI: 10.1006/abbi.1993.1009.
(21) Wortham, B. W.; Oliveira, M. A.; Patel, C. N. Polyamines in Bacteria: Pleiotropic Effects yet Specific Mechanisms. Springer New York, 2007; pp 106-115.
(22) Hasan, C. M.; Pottenger, S.; Green, A. E.; Cox, A. A.; White, J. S.; Jones, T.; Winstanley, C.; Kadioglu, A.; Wright, M. H.; Neill, D. R.; Fothergill, J. L. *Pseudomonas aeruginosa* utilizes the host-derived polyamine spermidine to facilitate antimicrobial tolerance. *JCI Insight* **2022**, *7* (22). DOI: 10.1172/jci.insight.158879.
(23) El-Halfawy, O. M.; Valvano, M. A. Chemical communication of antibiotic resistance by a highly resistant subpopulation of bacterial cells. *PLOS One* **2013**, *8* (7), e68874. DOI: 10.1371/journal.pone.0068874.
(24) El-Halfawy, O. M.; Valvano, M. A. Putrescine reduces antibiotic-induced oxidative stress as a mechanism of modulation of antibiotic resistance in *Burkholderia cenocepacia*. *Antimicrob Agents Chemother* **2014**, *58* (7), 4162-4171. DOI: AAC.02649-14.
(25) Kwon, D. H.; Lu, C. D. Polyamines induce resistance to cationic peptide, aminoglycoside, and quinolone antibiotics in *Pseudomonas aeruginosa* PAO1. *Antimicrob Agents Chemother* **2006**, *50* (5), 1615-1622.
(26) Kwon, D. H.; Lu, C. D. Polyamine effects on antibiotic susceptibility in bacteria. *Antimicrob Agents Chemother* **2007**, *51* (6), 2070-2077.
(27) El-Halfawy, O. M.; Valvano, M. A. Non-genetic mechanisms communicating antibiotic resistance: Rethinking strategies for antimicrobial drug design. *Expert Opinion On Drug Discovery* **2012**, *7* (10), 923-933.
(28) Vázquez-Laslop, N.; Mankin, A. S. How Macrolide Antibiotics Work. *Trends Biochem Sci* **2018**, *43* (9), 668-684. DOI: 10.1016/j.tibs.2018.06.011.
(29) Lalak, N. J.; Morris, D. L. Azithromycin clinical pharmacokinetics. *Clin Pharmacokinet* **1993**, *25* (5), 370-374. DOI: 10.2165/00003088-199325050-00003.
(30) Kohno, Y. Chapter 6 - Pharmacokinetics and Metabolism of Macrolides. In *Macrolide Antibiotics (Second Edition)*, Ōmura, S. Ed.; Academic Press, 2003; pp 327-361.
(31) Magill, S. S.; O'Leary, E.; Ray, S. M.; Kainer, M. A.; Evans, C.; Bamberg, W. M.; Johnston, H.; Janelle, S. J.; Oyewumi, T.; Lynfield, R.; et al. Antimicrobial Use in US Hospitals: Comparison of Results From Emerging Infections Program Prevalence Surveys, 2015 and 2011. *Clin Infect Dis* **2021**, *72* (10), 1784-1792. DOI: 10.1093/cid/ciaa373.
(32) Wilson, D. N. The A–Z of bacterial translation inhibitors. *Critical Reviews in Biochemistry and Molecular Biology* **2009**, *44* (6), 393-433. DOI: 10.3109/10409230903307311.
(33) Farha, M. A.; French, S.; Stokes, J. M.; Brown, E. D. Bicarbonate Alters Bacterial Susceptibility to Antibiotics by Targeting the Proton Motive Force. *ACS Infectious Diseases* **2018**, *4* (3), 382-390. DOI: 10.1021/acsinfecdis.7b00194.
(34) Ramage, B.; Erolin, R.; Held, K.; Gasper, J.; Weiss, E.; Brittnacher, M.; Gallagher, L.; Manoil, C. Comprehensive Arrayed Transposon Mutant Library of Klebsiella pneumoniae Outbreak Strain KPNIH1. *J Bacteriol* **2017**, *199* (20). DOI: 10.1128/JB.00352-17 From NLM PubMed-not-MEDLINE.
(35) CLSI. Performance Standards for Antimicrobial Susceptibility Testing. *CLSI supplement M100* **2020**, *30th ed.* .
(36) Thurlow, L. R.; Joshi, G. S.; Clark, J. R.; Spontak, J. S.; Neely, C. J.; Maile, R.; Richardson, A. R. Functional modularity of the arginine catabolic mobile element contributes to the success of USA300 methicillin-resistant *Staphylococcus aureus*. *Cell Host Microbe* **2013**, *13* (1), 100-107. DOI: 10.1016/j.chom.2012.11.012.

(37) Sagar, N. A.; Tarafdar, S.; Agarwal, S.; Tarafdar, A.; Sharma, S. Polyamines: Functions, Metabolism, and Role in Human Disease Management. *Med Sci (Basel)* **2021**, *9* (2). DOI: 10.3390/medsci9020044.
(38) Martin, M. J.; Stribling, W.; Ong, A. C.; Maybank, R.; Kwak, Y. I.; Rosado-Mendez, J. A.; Preston, L. N.; Lane, K. F.; Julius, M.; Jones, A. R.; et al. A panel of diverse *Klebsiella pneumoniae* clinical isolates for research and development. *Microb Genom* **2023**, *9* (5). DOI: 10.1099/mgen.0.000967.
(39) Liu, A.; Tran, L.; Becket, E.; Lee, K.; Chinn, L.; Park, E.; Tran, K.; Miller, J. H. Antibiotic sensitivity profiles determined with an *Escherichia coli* gene knockout collection: generating an antibiotic bar code. *Antimicrob Agents Chemother* **2010**, *54* (4), 1393-1403. DOI: 10.1128/AAC.00906-09.
(40) Izquierdo, L.; Coderch, N.; Pique, N.; Bedini, E.; Corsaro, M. M.; Merino, S.; Fresno, S.; Tomas, J. M.; Regue, M. The *Klebsiella pneumoniae wabG* gene: role in biosynthesis of the core lipopolysaccharide and virulence. *J Bacteriol* **2003**, *185* (24), 7213-7221. DOI: 10.1128/JB.185.24.7213-7221.2003.
(41) Furniss, R. C. D.; Kaderabkova, N.; Barker, D.; Bernal, P.; Maslova, E.; Antwi, A. A. A.; McNeil, H. E.; Pugh, H. L.; Dortet, L.; Blair, J. M. A.; et al. Breaking antimicrobial resistance by disrupting extracytoplasmic protein folding. *Elife* **2022**, *11*. DOI: 10.7554/eLife.57974.
(42) Wang, J.; Ma, W.; Wang, Z.; Li, Y.; Wang, X. Construction and Characterization of an *Escherichia coli* Mutant Producing Kdo2-Lipid A. *Marine Drugs* **2014**, *12* (3), 1495-1511. DOI: 10.3390/md12031495.
(43) Kneidinger, B.; Marolda, C.; Graninger, M.; Zamyatina, A.; McArthur, F.; Kosma, P.; Valvano, M. A.; Messner, P. Biosynthesis Pathway of ADP-L-glycero-beta-D-manno-heptose in *Escherichia coli*. *Journal of Bacteriology* **2002**, *184* (2), 363-369. DOI: 10.1128/jb.184.2.363-369.2002.
(44) Regué, M.; Climent, N. R.; Abitiu, N.; Coderch, N. R.; Merino, S.; Izquierdo, L.; Altarriba, M.; TomáS, J. M. Genetic Characterization of the *Klebsiella pneumoniae waa* Gene Cluster, Involved in Core Lipopolysaccharide Biosynthesis. *Journal of Bacteriology* **2001**, *183* (12), 3564-3573. DOI: 10.1128/jb.183.12.3564-3573.2001.
(45) Yethon, J. A.; Heinrichs, D. E.; Monteiro, M. A.; Perry, M. B.; Whitfield, C. Involvement of *waaY*, *waaQ*, and *waaP* in the modification of *Escherichia coli* lipopolysaccharide and their role in the formation of a stable outer membrane. *J Biol Chem* **1998**, *273* (41), 26310-26316. DOI: 10.1074/jbc.273.41.26310.
(46) Vaara, M. Agents that increase the permeability of the outer membrane. *Microbiological Reviews* **1992**, *56* (3), 395-411. DOI: doi:10.1128/mr.56.3.395-411.1992.
(47) Meehan, B. M.; Landeta, C.; Boyd, D.; Beckwith, J. The Disulfide Bond Formation Pathway Is Essential for Anaerobic Growth of *Escherichia coli*. *J Bacteriol* **2017**, *199* (16). DOI: 10.1128/jb.00120-17.
(48) Onufryk, C.; Crouch, M. L.; Fang, F. C.; Gross, C. A. Characterization of six lipoproteins in the sigmaE regulon. *J Bacteriol* **2005**, *187* (13), 4552-4561. DOI: 10.1128/jb.187.13.4552-4561.2005.
(49) Sykes, M. T.; Williamson, J. R. A complex assembly landscape for the 30S ribosomal subunit. *Annu Rev Biophys* **2009**, *38*, 197-215. DOI: 10.1146/annurev.biophys.050708.133615.
(50) Bubunenko, M.; Korepanov, A.; Court, D. L.; Jagannathan, I.; Dickinson, D.; Chaudhuri, B. R.; Garber, M. B.; Culver, G. M. 30S ribosomal subunits can be assembled in vivo without primary binding ribosomal protein S15. *RNA* **2006**, *12* (7), 1229-1239. DOI: 10.1261/rna.2262106.
(51) Ginzburg, I.; Miskin, R.; Zamir, A. N-ethyl maleimide as a probe for the study of functional sites and conformations of 30 S ribosomal subunits. *Journal of Molecular Biology* **1973**, *79* (3), 481-494. DOI: https://doi.org/10.1016/0022-2836(73)90400-2.
(52) Delvillani, F.; Papiani, G.; Deho, G.; Briani, F. S1 ribosomal protein and the interplay between translation and mRNA decay. *Nucleic Acids Res* **2011**, *39* (17), 7702-7715. DOI: 10.1093/nar/gkr417.
(53) Soh, S. M.; Jang, H.; Mitchell, R. J. Loss of the lipopolysaccharide (LPS) inner core increases the electrocompetence of *Escherichia coli*. *Appl Microbiol Biotechnol* **2020**, *104* (17), 7427-7435. DOI: 10.1007/s00253-020-10779-6.

662 (54) Sporing, I.; Felgner, S.; Preusse, M.; Eckweiler, D.; Rohde, M.; Haussler, S.; Weiss, S.; Erhardt, M.
663 Regulation of Flagellum Biosynthesis in Response to Cell Envelope Stress in *Salmonella enterica Serovar*
664 Typhimurium. *mBio* **2018**, *9* (3). DOI: 10.1128/mBio.00736-17.
665 (55) Frirdich, E.; Bouwman, C.; Vinogradov, E.; Whitfield, C. The Role of Galacturonic Acid in Outer
666 Membrane Stability in *Klebsiella pneumoniae*. *Journal of Biological Chemistry* **2005**, *280* (30), 27604-
667 27612. DOI: 10.1074/jbc.m504987200.
668 (56) Al-Marzooq, F.; Ghazawi, A.; Tariq, S.; Daoud, L.; Collyns, T. Discerning the role of polymyxin B
669 nonapeptide in restoring the antibacterial activity of azithromycin against antibiotic-resistant *Escherichia*
670 *coli*. *Front Microbiol* **2022**, *13*, 998671. DOI: 10.3389/fmicb.2022.998671.
671 (57) Wesseling, C. M. J.; Martin, N. I. Synergy by Perturbing the Gram-Negative Outer Membrane:
672 Opening the Door for Gram-Positive Specific Antibiotics. *ACS Infectious Diseases* **2022**, *8* (9), 1731-1757.
673 DOI: 10.1021/acsinfecdis.2c00193.
674 (58) Rosner, J. L.; Martin, R. G. Reduction of cellular stress by TolC-dependent efflux pumps in
675 *Escherichia coli* indicated by BaeSR and CpxARP activation of spy in efflux mutants. *J Bacteriol* **2013**, *195*
676 (5), 1042-1050. DOI: 10.1128/JB.01996-12.
677 (59) Li, J.; Beuerman, R.; Verma, C. S. Mechanism of polyamine induced colistin resistance through
678 electrostatic networks on bacterial outer membranes. *Biochim Biophys Acta Biomembr* **2020**, *1862* (9),
679 183297. DOI: 10.1016/j.bbamem.2020.183297.
680 (60) Siegal-Gaskins, D.; Tuza, Z. A.; Kim, J.; Noireaux, V.; Murray, R. M. Gene circuit performance
681 characterization and resource usage in a cell-free "breadboard". *ACS Synth Biol* **2014**, *3* (6), 416-425.
682 DOI: 10.1021/sb400203p.
683 (61) Kanemura, A.; Yoshikawa, Y.; Fukuda, W.; Tsumoto, K.; Kenmotsu, T.; Yoshikawa, K. Opposite effect
684 of polyamines on In vitro gene expression: Enhancement at low concentrations but inhibition at high
685 concentrations. *PLoS One* **2018**, *13* (3), e0193595. DOI: 10.1371/journal.pone.0193595.
686 (62) Igarashi, K.; Kashiwagi, K. Effects of polyamines on protein synthesis and growth of *Escherichia coli*.
687 *Journal of Biological Chemistry* **2018**, *293* (48), 18702-18709. DOI: 10.1074/jbc.tm118.003465.
688 (63) Agrawal, R. K.; Penczek, P.; Grassucci, R. A.; Burkhardt, N.; Nierhaus, K. H.; Frank, J. Effect of buffer
689 conditions on the position of tRNA on the 70 S ribosome as visualized by cryoelectron microscopy. *J Biol*
690 *Chem* **1999**, *274* (13), 8723-8729. DOI: 10.1074/jbc.274.13.8723.
691 (64) Winther, K. S.; Sorensen, M. A.; Svenningsen, S. L. Polyamines are Required for tRNA Anticodon
692 Modification in *Escherichia coli*. *J Mol Biol* **2021**, *433* (15), 167073. DOI: 10.1016/j.jmb.2021.167073.
693 (65) Dever, T. E.; Ivanov, I. P. Roles of polyamines in translation. *Journal of Biological Chemistry* **2018**,
694 *293* (48), 18719-18729. DOI: 10.1074/jbc.tm118.003338.
695 (66) Amarantos, I.; Zarkadis, I. K.; Kalpaxis, D. L. The identification of spermine binding sites in 16S rRNA
696 allows interpretation of the spermine effect on ribosomal 30S subunit functions. *Nucleic Acids Res* **2002**,
697 *30* (13), 2832-2843. DOI: 10.1093/nar/gkf404.
698 (67) Kalpaxis, D. L.; Drainas, D. Inhibitory effect of spermine on ribosomal peptidyltransferase. *Arch*
699 *Biochem Biophys* **1993**, *300* (2), 629-634. DOI: 10.1006/abbi.1993.1087.
700 (68) Teraoka, H.; Tanaka, K. Effect of Spermine on the Binding of Erythromycin to *Escherichia coli*
701 Ribosomes and the Peptidyl-Transfer Reaction. *European Journal of Biochemistry* **1973**, *33* (3), 578-583.
702 DOI: 10.1111/j.1432-1033.1973.tb02718.x.
703 (69) Chopra, I.; Roberts, M. Tetracycline Antibiotics: Mode of Action, Applications, Molecular Biology,
704 and Epidemiology of Bacterial Resistance. *Microbiology and Molecular Biology Reviews* **2001**, *65* (2),
705 232-260. DOI: 10.1128/mmbr.65.2.232-260.2001.
706 (70) Saiman, L.; Chen, Y.; Gabriel, P. S.; Knirsch, C. Synergistic activities of macrolide antibiotics against
707 *Pseudomonas aeruginosa, Burkholderia cepacia, Stenotrophomonas maltophilia,* and *Alcaligenes*
708 *xylosoxidans* isolated from patients with cystic fibrosis. *Antimicrob Agents Chemother* **2002**, *46* (4),
709 1105-1107.

710 (71) Wimberly, B. T.; White, S. W.; Ramakrishnan, V. The structure of ribosomal protein S7 at 1.9 A
711 resolution reveals a beta-hairpin motif that binds double-stranded nucleic acids. *Structure* **1997**, *5* (9),
712 1187-1198. DOI: 10.1016/s0969-2126(97)00269-4.
713 (72) Lennen, R. M.; Lim, H. G.; Jensen, K.; Mohammed, E. T.; Phaneuf, P. V.; Noh, M. H.; Malla, S.;
714 Borner, R. A.; Chekina, K.; Ozdemir, E.; et al. Laboratory evolution reveals general and specific tolerance
715 mechanisms for commodity chemicals. *Metab Eng* **2023**, *76*, 179-192. DOI:
716 10.1016/j.ymben.2023.01.012.
717 (73) Noah, J. W.; Dolan, M. A.; Babin, P.; Wollenzien, P. Effects of Tetracycline and Spectinomycin on the
718 Tertiary Structure of Ribosomal RNA in the *Escherichia coli* 30 S Ribosomal Subunit. *Journal of Biological*
719 *Chemistry* **1999**, *274* (23), 16576-16581. DOI: 10.1074/jbc.274.23.16576.
720 (74) Svensson, P.; Changchien, L. M.; Craven, G. R.; Noller, H. F. Interaction of ribosomal proteins, S6, S8,
721 S15 and S18 with the central domain of 16 S ribosomal RNA. *J Mol Biol* **1988**, *200* (2), 301-308. DOI:
722 10.1016/0022-2836(88)90242-2.
723 (75) Buttin, G.; Cohen, G. N.; Monod, J.; Rickenberg, H. V. Galactoside-permease of *Escherichia coli*. *Ann*
724 *Inst Pasteur (Paris)* **1956**, *91* (6), 829-857.
725 (76) Bolivar, F.; Rodriguez, R. L.; Greene, P. J.; Betlach, M. C.; Heyneker, H. L.; Boyer, H. W.; Crosa, J. H.;
726 Falkow, S. Construction and characterization of new cloning vehicles. II. A multipurpose cloning system.
727 *Gene* **1977**, *2* (2), 95-113. DOI: 0378-1119(77)90000-2 [pii].
728 (77) CLSI. *Methods for Dilution Antimicrobial Susceptibility Tests for Bacteria That Grow Aerobically;*
729 *Approved Standard—Ninth Edition. CLSI document M07-A9.*; Clinical and Laboratory Standards Institute,
730 2012.
731 (78) Hancock, R. E.; Wong, P. G. Compounds which increase the permeability of the *Pseudomonas*
732 *aeruginosa* outer membrane. *Antimicrob Agents Chemother* **1984**, *26* (1), 48-52.
733 (79) Farha, M. A.; El-Halfawy, O. M.; Gale, R. T.; MacNair, C. R.; Carfrae, L. A.; Zhang, X.; Jentsch, N. G.;
734 Magolan, J.; Brown, E. D. Uncovering the hidden antibiotic potential of Cannabis. *ACS Infect Dis* **2020**, *6*
735 (3), 338-346. DOI: 10.1021/acsinfecdis.9b00419.

736